Surface & Coatings Technology 205 (2010) 2585–2589

Contents lists available at ScienceDirect

Surface & Coatings Technology

journal homepage: www.elsevier.com/locate/surfcoat

Investigation of $Co(OH)_2$ formation during cobalt electrodeposition using a chemometric procedure

J.S. Santos, F. Trivinho-Strixino, E.C. Pereira *

NANOFAEL, CMDMC, Departamento de Química, Universidade Federal de São Carlos, Cx. 676, São Carlos, SP, Brazil

ARTICLE INFO

Article history:
Received 5 March 2010
Accepted in revised form 2 October 2010
Available online 1 November 2010

Keywords:
Cobalt electrodeposition
Cobalt hydroxide
EQCM
Factorial design
Chemometric

ABSTRACT

The mechanism of Co electrodeposition in sulphate solutions containing boric acid was investigated using the EQCM technique and potentiostatic measurements. The effects of solution composition, temperature and deposition potential were studied using factorial design as a chemometric procedure. The boric acid was used as a buffer to prevent pH changes due to the hydrogen evolution reaction (HER) during electrodeposition. The results showed that $Co(OH)_2$ was formed as a parallel reaction to metallic Co formation under some experimental conditions. The analysis of the factorial design revealed that temperature and $[Co^{2+}:H_3BO_3]$ molar ratio were the critical variables that affect the mechanism of cobalt electrodeposition. At high temperatures (48 °C) and using a 5:1 molar ratio of $[Co^{2+}:H_3BO_3]$, the formation of cobalt hydroxide was detected simultaneously with cobalt deposition.

1. Introduction

During cobalt electrodeposition in an aqueous solution, hydrogen evolution occurs as a parallel process that consumes part of the applied current and reduces the overall process efficiency. This secondary process can affect the pH at the electrode–electrolyte interface and also modifies the kinetics and mechanism of cobalt electrodeposition [1–4]. As a consequence, the local pH rise can lead to cobalt hydroxide precipitation over the electrode, which interferes with the formation of the metallic deposit producing a porous structure [5–8]. The increase of pH near the electrode surface occurs due to water electrolysis and the hydrogen evolution reaction (HER) [2,9], which is described as follows:

$$H_2O + M{-}H + e^- \rightarrow M + H_2(ads) + OH^-. \qquad (1)$$

In order to avoid the pH variation at the electrode surface during the electrochemical process, boric acid (H_3BO_3) is usually added to the electrolyte [10–16]. As a result, the formation of hydroxide species should be inhibited. Regardless, the real function of this additive in the electrodeposition is controversial and different propositions have been considered [13–16].

Due to the reaction complexity, several mechanisms for cobalt electrodeposition have been regarded in the literature [3,5,9,17,18]. In general, these studies are potentiodynamic and the proposed mechanisms depend on the solution pH and involve the formation of intermediates, such as $CoOH^+$ and/or $Co(OH)_2$. In our previous study [4], we investigated the effect of the temperature on the Co electrodeposition mechanism in sulphate solutions containing boric acid during potentiostatic depositions using the Electrochemical Quartz Crystal Microbalance technique (EQCM). The parameter used to discuss the reaction mechanism was the apparent *M/z* value, a single factor which combines potentiostatic measurements and EQCM data [3,19]. The results showed that only metallic Co was deposited at 25 °C, whereas a large amount of $Co(OH)_2$ was detected at 48 °C. These results suggested that, under that condition, the buffer contribution of boric acid is not effective in the electrodeposition process. In order to verify if this behavior can be observed in other experimental conditions, the study was extended and a factorial design was used to optimize the experiments and analyze the data [20,21]. The potential advantages of using this chemometric procedure are to reduce the number of experiments that must be performed and to quantify the effects of each parameter and their cross-effects related to a specific parameter [20,21]. The parameter chosen to investigate the Co electrodeposition mechanism change is the same from our previous work, i.e. the *M/z* ratio. The new set of results showed that not only the temperature affects the mechanism of Co electrodeposition, as observed in our previous work [4], but also the effect of the $[Co^{2+}:H_3BO_3]$ molar ratio on the *M/z* response is significant. Moreover, the chemometric analysis reveals that the cross-effect of the temperature and molar ratio is critical in this electrochemical process and a mixed mechanism can occur if these both parameters are changed simultaneously.

2. Experimental

2.1. Electrochemical measurements

The experiments were carried out in a glass cell maintained at a constant temperature using a thermostatic bath. The working electrode

---

* Corresponding author. Tel.: +55 16 3351 9309; fax: +55 16 33518214.
E-mail address: decp@power.ufscar.br (E.C. Pereira).

0257-8972
doi:10.1016/j.surfcoat.2010.10.005

(WE) was a 9 MHz AT-cut quartz crystal which exhibits excellent frequency *vs*. temperature stability [22]. This crystal is coated with a Pt film covering a geometric area equal to 0.2 cm^2. The auxiliary electrode (AE) was a Pt sheet and all potentials were referenced to a saturated calomel electrode (SCE). The resonance frequency shift was measured with a Seiko EG&G Quartz Crystal Microbalance (model QCA 917) and the system sensitivity coefficients (*K*) were determined by calibration [23]. The obtained values were 858.8 Hz μg^{-1} and 942.6 Hz μg^{-1} at 25 °C and 48 °C, respectively. The electrochemical measurements were conducted using an EG&G PAR 263A potentiostat/galvanostat and two electrolytes were used: 0.01 M $CoSO_4$ + 0.01 M H_3BO_3 + 0.17 M Na_2SO_4 (pH 5.3) and 0.05 M $CoSO_4$ + 0.01 M H_3BO_3 + 0.11 M Na_2SO_4 (pH 5.2), with Na_2SO_4 as a supporting electrolyte and also to maintain ionic strength constant. All solutions were prepared with deionised water and analytical-grade reagents. Before each experiment, the electrolyte solution was bubbled with N_2 flux for 20 min.

2.2. Factorial design

The calculated effects using a factorial design are determined by a matrix calculation merging all variables at their different values [20,21]. In this procedure, k^n experiments must be accomplished, where *n* is the number of variables or parameters and *k* is the number of values of each variable. Then to perform a factorial design with three variables and two values, eight experiments are needed ($2^3 = 8$ experiments). In this study, a 2^3 factorial design was used, where the parameters chosen were [Co^{2+}:H_3BO_3] molar ratio, temperature and deposition potential. These variables were studied at two fixed values, where the lowest was indicated by (−) and the highest by (+). In this case, the response used to quantify the effects of the variables was the *M*/*z* ratio, which was calculated considering the mass variation and charge during the measurements [3,4]. In the factorial design matrix, the parameters and values used are described in Table 1. The experiments were performed in duplicate and a Student's *t*-distribution with 8 degrees of freedom and 95% confidence interval was used to calculate the experimental error associated with individual responses [20,21]. A detailed description concerning the calculation procedure of the effects and their standard error for a 2^3 factorial design can be found elsewhere [21].

2.3. EQCM data processing

The EQCM technique coupled with electrochemical experiments is a convenient tool to investigate an electrochemical reaction by simultaneously measuring the current, charge and mass variation at the working electrode. According to the Sauerbrey equation [24], the observed resonant frequency shift (Δf) can be converted to mass change (Δm) following:

$$\Delta f = K . \Delta m.$$

This equation is valid if the deposits are rigid and slip conditions are not met [22,25]. In the present case, the cobalt deposits are rigid and satisfied those conditions, however, careful attention should be made to avoid wrong interpretation of results. According to some authors [25,26], the frequency change induced by immersion in an electrolyte is related to the density and viscosity of the solution. Therefore, if electrolyte temperature changes the sensitivity coefficient may change either. For this reason, the sensitivity coefficient was determined by calibration prior to the experiments at 25° and 48 °C as described above.

Table 1
2^3 factorial design matrix combining all variables and values.

Variables	Values (−)	Values (+)	Exp.	A	B	C
			1	−	−	−
(A) [Co^{2+}: H_3BO_3] molar ratio	1:1	5:1	2	+	−	−
(B) Temperature (°C)	25	48	3	−	+	−
(C) E_{dep} (V)	−0.90	−0.95	4	+	+	−
			5	−	−	+
			6	+	−	+
Response: *M*/*z* (g mol^{-1})			7	−	+	+
			8	+	+	+

As discussed in previous works [3,4,19], the relationship between apparent molar mass and the number of electrons involved in the reaction (*M*/*z*) can be obtained by the product of the Faraday constant and the derivative of the mass *vs*. charge curve using the mass variation data and the Faraday Law. The *M*/*z* values can be used to evaluate the number of reactions occurring simultaneously during an electrochemical process. In the present study, the *M*/*z* values were calculated from potentiostatic depositions at −0.90 V and −0.95 V for 10 s in $CoSO_4$ solutions containing boric acid at two fixed temperatures (25 °C and 48 °C). These experimental conditions are used according to the 2^3 factorial design presented in Table 1.

3. Results and discussion

Fig. 1 exhibits the current transients obtained during potentiostatic electrodeposition of cobalt in sulphate solutions and the corresponding mass change observed during the process. In these experiments, a step potential was applied between −0.1 V (where no Faradaic reaction occurs) and −0.90 V or −0.95 V for 10 s at 25 °C or 48 °C. The experimental conditions were chosen combining all variables and values presented in Table 1. The results showed that the current related to the experiments performed in solutions containing [Co^{2+}:H_3BO_3] in a molar ratio of 5:1 (Fig. 1B) was higher than those observed in solutions which the molar ratio used was 1:1 (Fig. 1A), except for deposition at *E* = −0.90 V and 25 °C. In the last case, the currents for both molar ratios have similar values. Besides, it was also observed that the deposited mass was higher in solutions containing [Co^{2+}:H_3BO_3] in a molar ratio of 5:1 (compares Fig. 1C and D). This increase in absolute mass and total current at molar ratio of 5:1 is related to the higher Co content in the electrolyte increasing the rate of Co metal deposition.

In order to study the effects of the variables on the mechanism of cobalt electrodeposition, the relation between molar mass and the number of electrons involved in the reaction (*M*/*z*) was calculated and compared with the theoretical values. At first, some assumptions need to be made to determine which species are present at any stage of the deposition. The *M*/*z* value involving direct cobalt reduction is 29.5 g mol^{-1} (MW Co/$2e^-$ = 58.9 g mol^{-1}), according to the reaction:

$$Co^{2+}(aq) + 2e^- \rightarrow Co(s). \quad (2)$$

On the other hand, the *M*/*z* value corresponding to $Co(OH)_2$ formation is 46.5 g mol^{-1} (MW $Co(OH)_2$/$2e^-$), in accordance with the global reaction obtained from Eqs. (3) and (4):

$$2H_2O + 2e^- \rightarrow H_2(g) + 2OH^-(aq) \quad (3)$$

$$Co^{2+}(aq) + 2OH^-(aq) \rightarrow Co(OH)_2(ads) \quad (4)$$

Comparing these theoretical *M*/*z* values with the experimental ones, it is possible to distinguish the mechanism of cobalt electrodeposition and evaluate when a mixed mechanism occurs during the electrochemical process. During cobalt electrodeposition, experimental *M*/*z* values close to the theoretical value of 29.5 g mol^{-1}, indicate that the direct Co metallic deposition is the dominant mechanism (Eq. 2). For experimental *M*/*z* values close to 46.5 g mol^{-1}, the mechanism of $Co(OH)_2$ formation is the most important (Eqs. 3 and 4). In addition, experimental *M*/*z* values between 29.5 and 46.5 g mol^{-1} suggest that both mechanisms occur simultaneously and their magnitude gives the proportion of each reaction.

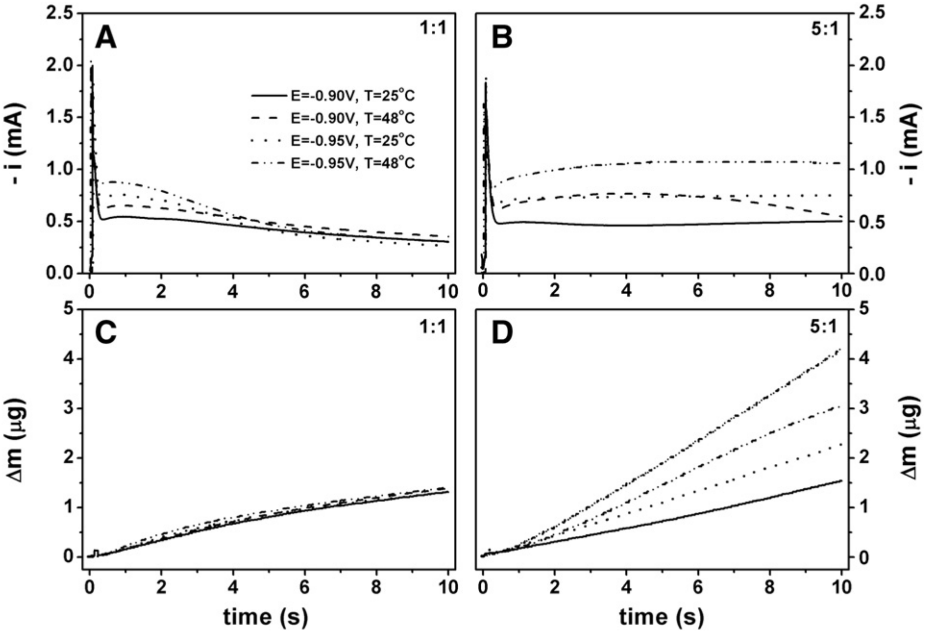

Fig. 1. Cobalt potentiostatic depositions and mass variation during the experiments performed in sulphate solution containing [Co^{2+}:H_3BO_3] in a molar ratio of 1:1 and 5:1.

It is important to stress that $Co(OH)_2$ reduction to metallic Co occurs at more negative potentials, following:

$$Co(OH)_2(ads) + 2e^- \rightarrow Co(s) + 2OH^-(aq). \quad (5)$$

The Standard Potential for Eq. (5) is −0.97 V *vs.* SCE [5,27] and the mechanism for the $Co(OH)_2$ reduction involving reactions (3)–(5) require an apparent *M/z* value of 14.7 g mol^{-1} (MW Co/4e^-). In this study, the potentials used for cobalt potentiostatic deposition were more positive than −0.97 V and were located close to the water electrolysis potential where HER occurs. Therefore, the majority of $Co(OH)_2$ produced is not reduced to Co(s) using these experimental conditions.

The apparent *M/z* values as a function of deposition time for each experiment are shown in Fig. 2. In this figure, it was observed that the *M/z* values approach 29 g mol^{-1} at 10 s for all experiments performed at 25 °C indicating that the major reaction is described by Eq. (2), *i.e.* direct cobalt deposition involving 2 mol of electrons ($M_{Co}/2e^- = 29.5$ g $\text{mol}^{>-1}$). Consequently, only metallic Co was produced on the electrode independent of [Co^{2+}:H_3BO_3] molar ratio. In addition, from inspection of Fig. 2(A) and (C), similar results are observed for the deposition carried out at 48 °C and in the solution containing a [Co^{2+}:H_3BO_3] in a molar ratio of 1:1. In these cases, the *M/z* values also approach 29 g mol^{-1} at 10 s, which also suggests that the dominant mechanism is the direct cobalt deposition. On the other hand, different behaviour can be observed during the potentiostatic deposition at 48 °C in the electrolyte containing a [Co^{2+}:H_3BO_3] in a molar ratio of 5:1 (Fig. 2B and D). In these cases, during early stages of deposition, *M/z* values are close to 29 g mol^{-1}. However, as long as deposition proceeds, the *M/z* values increase to 41.9 ± 0.5 g mol^{-1} and 39.1 ± 0.5 g mol^{-1}, during depositions at −0.90 V and −0.95 V, respectively. These *M/z* values are related to $Co(OH)_2$ formation according to the global reaction originated from Eqs. (3) and (4). Furthermore, the

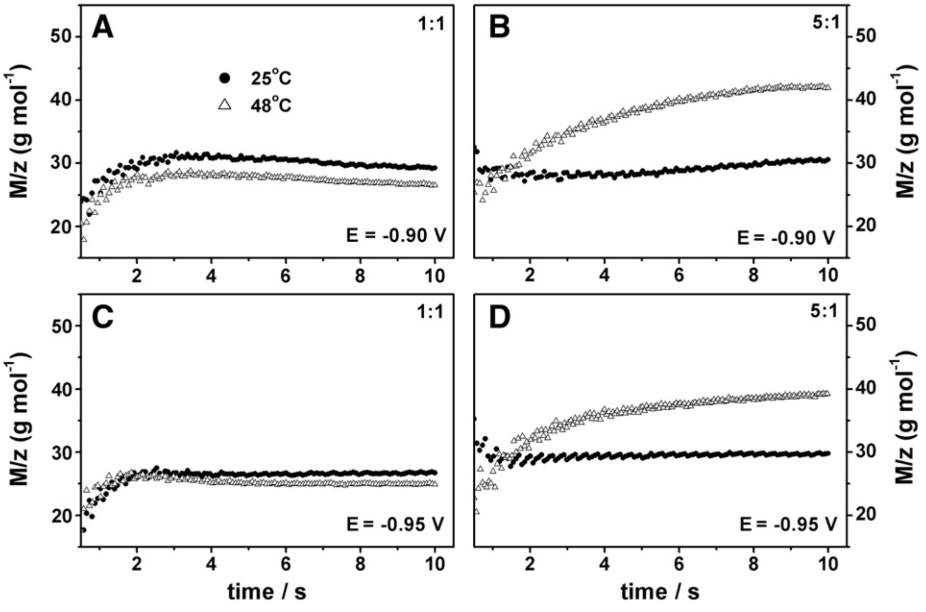

Fig. 2. *M/z* transients as a function of time during cobalt potentiostatic depositions.

lowest experimental *M/z* value compared to the theoretical ones for deposition at −0.95 V is expected since $Co(OH)_2$ could be reduced to Co (s) at more negative potentials during the electrodeposition process [5,27]. In summary, these results reveal that, besides the temperature, the electrolyte composition can also affect the mechanism of cobalt electrodeposition.

To study the electrodeposition process in a more detailed way, these results are combined in a 2^3 factorial design performed in duplicate, where the responses used to quantify the effect of the variables were the *M/z* mean values at $t = 2$ s and $t = 10$ s, *i.e.* during the early stages of the cobalt deposition and at the end of the experiment. Fig. 3 shows the geometric representation of the results for all experimental conditions performed at $t = 2$ s and $t = 10$ s. In this scheme, *M/z* mean values are located at the corner of the cube in which the axes represent the variables investigated: $[Co^{2+}:H_3BO_3]$ molar ratio, temperature and deposition potential. As can be observed in Fig. 3, the *M/z* mean values at 2 s and 10 s are close to 29 g mol^{-1} in almost all experimental conditions, except for those obtained at 10 s during depositions performed at 48 °C in the electrolyte containing $[Co^{2+}:H_3BO_3]$ in a molar ratio of 5:1 (Fig. 3B). These results demonstrate that the Co electrodeposition mechanism changes in these last conditions. Moreover, the change in the calculated *M/z* values from 2 to 10 s indicates an accumulation process consistent with a pH increase in the solution near the interface since the *M/z* values increase from 31.8 to 41.9 g mol^{-1} at −0.90 V and 32.3 to 39.1 g mol^{-1} at −0.95 V.

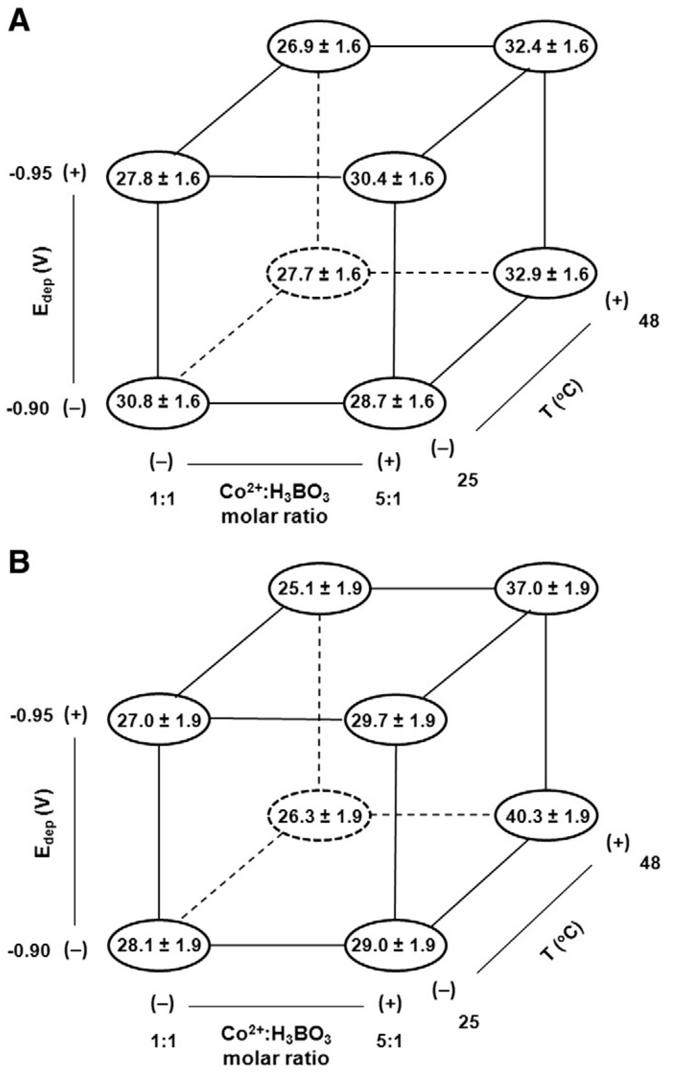

Fig. 3. Geometric representation of *M/z* mean values (g mol^{-1}) at (A) $t = 2$ s and (B) $t = 10$ s.

The average of the *M/z* values for all experiments, the main effects of the variables corresponding to *M/z* response at $t = 2$ s and $t = 10$ s of deposition and the interaction effects between two and three variables are presented in Table 2. A better visualization of these results is depicted in the Pareto diagrams in Fig. 4. In these diagrams, the effects for the *M/z* response at the end of the deposition are plotted in increasing order and its values are standardized by an associated error (denoted in this figure by a straight vertical line) [20]. Note that the $[Co^{2+}:H_3BO_3]$ molar ratio and temperature are the most important factors that affect the *M/z* response and there is a high interaction effect between these variables. Also, it can be seen that the other parameters and their interaction effects are small and can be neglected from the analysis because they are smaller than the associated error.

From Table 2, the analysis of the main effect from the solution composition shows that the *M/z* values can increase 2.8 ± 1.6 g mol^{-1} during the early stages of deposition ($t = 2$ s) and 7.4 ± 1.9 g mol^{-1} at the end of the process ($t = 10$ s) if the $[Co^{2+}:H_3BO_3]$ molar ratio is changed from 1:1 to 5:1. This increase of the *M/z* responses indicates a mechanism change in the cobalt deposition process, meaning that $Co(OH)_2$ can form simultaneously with the metallic Co electrodeposition. Moreover, the effect of solution composition reveals that $Co(OH)_2$ accumulates over the cobalt deposits since the *M/z* response can increase from 2.8 g mol^{-1} to 7.4 g mol^{-1} as long as the deposition proceeds, which denotes the accumulation effects inferred from Fig. 2.

Table 2 also shows the main effect from the temperature change. It was observed that this effect is not significant during the early stages of deposition, because the *M/z* value at 2 s is smaller than the standardized error and can be neglected. On the other hand, the increase of 3.7 ± 1.9 g mol^{-1} in *M/z* response at 10 s suggests that the temperature also affects the mechanism of cobalt electrodeposition as long as the deposition proceeds leading to a mixed mechanism if the electrolyte temperature is changed from 25 °C to 48 °C.

Regarding the main effect of potential deposition, it can be observed in Table 2 that the effect for both cases is smaller than standardized error and can be neglected then in these experimental conditions.

From the analysis of the cross-effects, it was observed that the interaction effect between $[Co^{2+}:H_3BO_3]$ molar ratio and temperature is critical, showing a positive effect of 2.5 ± 1.6 g mol^{-1} and 5.6 ± 1.9 g mol^{-1} for $t = 2$ s and $t = 10$ s, respectively. These results indicate that both variables are truly responsible for the mixed mechanism observed in these conditions. Note that in Fig. 2A, the change of the temperature did not affect the mechanism of cobalt deposition when a $[Co^{2+}:H_3BO_3]$ molar ratio of 1:1 was used. However, there is a mechanism change in potentiostatic deposition at a high temperature if a $[Co^{2+}:H_3BO_3]$ in a molar ratio of 5:1 is used (Fig. 2B).

To summarize, these results showed that the $[Co^{2+}:H_3BO_3]$ molar ratio and temperature are critical factors that can affect the mechanism of the cobalt electrodeposition process leading to a mixed mechanism. Moreover, the effectiveness of the H_3BO_3 additive in certain experimental conditions is demonstrated. This situation occurs when the $[Co^{2+}:H_3BO_3]$

Table 2
Variable effects estimated for 2^3 factorial design results.

	Estimate of variable effects (g mol^{-1})	
	$t = 2$ s	$t = 10$ s
Average ± SD	29.7 ± 0.8	30.3 ± 1.0
Main effects ± SD		
(A) Molar ratio	2.8 ± 1.6	7.4 ± 1.9
(B) Temperature	0.6 ± 1.6	3.7 ± 1.9
(C) Deposition potential	−0.7 ± 1.6	−1.3 ± 1.9
Interaction of two-factors ± SD		
(A) × (B)	2.5 ± 1.6	5.6 ± 1.9
(A) × (C)	1.2 ± 1.6	−0.1 ± 1.9
(B) × (C)	−0.1 ± 1.6	−1.1 ± 1.9
Interaction of three-factors ± SD		
(A) × (B) × (C)	−1.1 ± 1.6	−1.0 ± 1.9

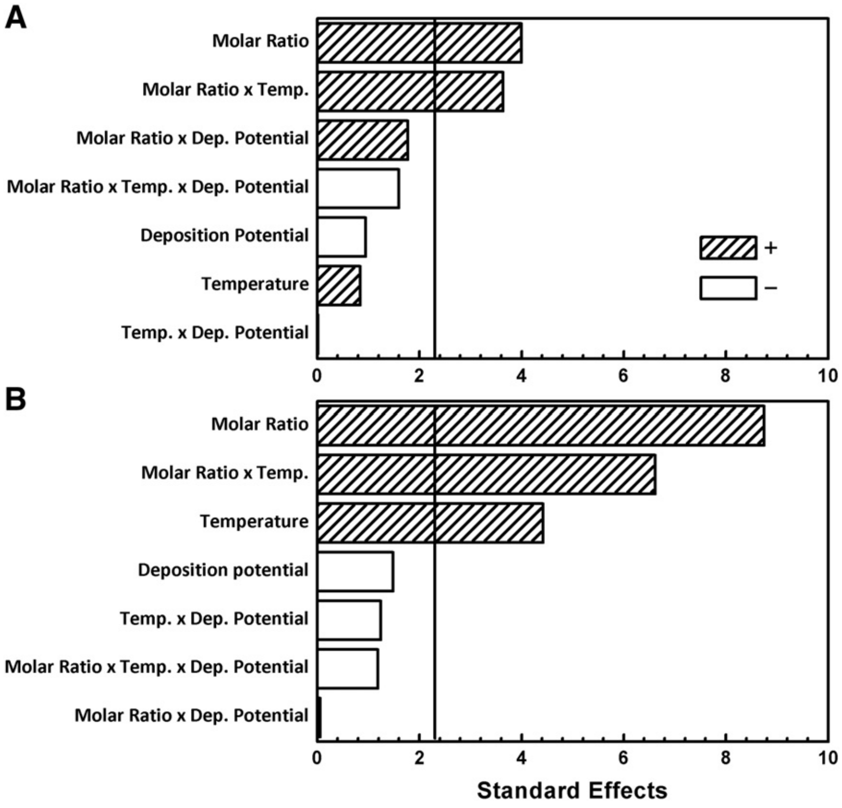

Fig. 4. Pareto Diagram for *M/z* response at (A) $t = 2$ s and (B) $t = 10$ s.

molar ratio is 1:1 at both temperatures investigated: 25 °C and 48 °C. In the case of potentiostatic depositions performed using [Co^{2+}:H_3BO_3] in a molar ratio of 5:1, the formation of $Co(OH)_2$ can occur simultaneously with metallic Co deposition if the temperature is changed from 25 °C to 48 °C. An explanation for these changes can be offered as follows: Jeffrey et al. [17] and Elsherief [28] proposed that HER contribution is intense in experiments performed at high temperatures. If we consider that the hydrogen evolution reaction is more effective at 48 °C, the reaction rate of water electrolysis in this condition must be higher than the experiments carried out at 25 °C. As a consequence, the OH^- concentration at the electrode interface must be higher at 48 °C than 25 °C. This fact explains the *M/z* values observed for hydroxylate species in experiments 4 and 8 (Table 1), in which the [Co^{2+}:H_3BO_3] molar ratio is 5:1. However, this individual argument does not explain the *M/z* values observed in experiments 3 and 7 (Table 1), in which the [Co^{2+}:H_3BO_3] molar ratio is 1:1 and $T = 48$ °C. In this case, we suggest that the quantity of Co^{2+} ions in the solution is not high enough to cause $Co(OH)_2$ precipitation [29] during the reaction, since the effect of the molar ratio combined with the temperature is critical.

4. Conclusions

The analysis of EQCM data coupled with potentiostatic measurements indicated that the mechanism of cobalt electrodeposition can change depending on the variables used during the deposition process in sulphate solution containing boric acid. The chemometric analysis using the factorial design showed that temperature and solution composition are critical parameters that significantly affect the mechanism of cobalt potentiostatic deposition. From the experimental conditions used here, the results showed that the cobalt electrodeposition can be characterized by a mixed mechanism, *i.e.*, a $Co(OH)_2$ precipitation over the electrode occurring simultaneously with direct cobalt reduction when the electrodeposition is carried out at a high temperature (48 °C) and the [Co^{2+}:H_3BO_3] molar ratio is 5:1.

Acknowledgments

The authors are grateful to CNPq and Capes for the financial support.

References

[1] P. Vermeiren, R. Leysen, H. Vandenborre, Electrochim. Acta 30 (1985) 1253.
[2] D.R. Gabe, J. Appl. Electrochem. 27 (1997) 908.
[3] J.T. Matsushima, F. Trivinho-Strixino, E.C. Pereira, Electrochim. Acta 51 (2006) 1960.
[4] J.S. Santos, R. Matos, F. Trivinho-Strixino, E.C. Pereira, Electrochim. Acta 53 (2007) 644.
[5] S.P. Jiang, A.C.C. Tseung, J. Electrochem. Soc. 137 (1990) 3387.
[6] S. Nakahara, S. Mahajan, J. Electrochem. Soc. 127 (1980) 283.
[7] H.L. Gaigher, N.G. van der Berg, Electrochim. Acta 21 (1976) 45.
[8] A. Ursache, J.T. Goldbach, T.P. Russell, M.I. Tuominen, J. Appl. Phys. 97 (2005) 10J322.
[9] N. Pradhan, T. Subbaiah, S.C. Das, U.N. Dash, J. Appl. Electrochem. 27 (1997) 713.
[10] N. Zech, D. Landolt, Electrochim. Acta 45 (2000) 3461.
[11] J. Ji, W.C. Cooper, D.B. Dreisinger, E. Peters, J. Appl. Electrochem. 25 (1995) 642.
[12] B.C. Tripathy, P. Singh, D.M. Muir, Metall. Mater. Trans. B 32 (2001) 395.
[13] J.P. Hoare, J. Electrochem. Soc. 133 (1986) 2491.
[14] J. Horkans, J. Electrochem. Soc. 126 (1979) 1861.
[15] K.-M. Yin, B.-T. Lin, Surf. Coat. Technol. 78 (1996) 205.
[16] B.V. Tilak, A.S. Gendron, M.A. Mosoiu, J. Appl. Electrochem. 7 (1977) 495.
[17] M.I. Jeffrey, W.L. Choo, P.L. Breuer, Miner. Eng. 13 (2000) 1231.
[18] M. Darques, L. Piraux, A. Encinas, IEEE Trans. Magn. 41 (2005) 3415.
[19] H.a.K.M. Saloniemi, M. Ritala, M. Leskela, J. Electroanal. Chem. 482 (2000) 139.
[20] G.E.P. Box, W.G. Hunter, J.S. Hunter, Statistic for Experiments: An Introduction to Design, Data Analysis, and Model Building, John Wiley & Sons, New York, 1978.
[21] E. Bruns, I.S. Scarminio, B. Barros Neto, Statiscal Design — Chemometrics, Elsevier Science, Amsterdan, 2006.
[22] M. Hepel, in: A. Wieckowski (Ed.), Interfacial Electrochemistry — Theory, Experiments and Applications, Marcel Dekker, New York, 1999.
[23] S. Bruckenstein, S. Swathirajan, Electrochim. Acta 30 (1985) 851.
[24] G. Sauerbrey, Z. Fur Phys. 155 (1959) 206.
[25] V. Tsionsky, L. Daikhin, M. Urbakh, E. Gileadi, in: A.J. Bard, I. Rubistein (Eds.), Electroanalytical Chemistry — A Series of Advances, vol. 22, Marcel Dekker, New York, 2004.
[26] K.K. Kanazawa, J.G. Gordon, Anal. Chem. 57 (1985) 1770.
[27] D.R. Lide, CRC Handbook of Chemistry and Physics, CRC Press, Florida, 1992.
[28] A.E. Elsherief, J. Appl. Electrochem. 33 (2003) 43.
[29] K. Higashi, H. Fukushima, T. Urakawa, T. Adaniya, K. Matsudo, J. Electrochem. Soc. 128 (1981) 2081.